Proc. Natl. Acad. Sci. USA
Vol. 77, No. 8, pp. 4904–4908, August 1980
Immunology

Fluorescence immunoassay based on long time correlations of number fluctuations

(diffusion/intensity autocorrelation/human IgG assay/microcomputer-based instrument)

D. F. NICOLI, J. BRIGGS†, AND V. B. ELINGS

Department of Physics, University of California, Santa Barbara, California 93106

Communicated by George Feher, April 7, 1980

ABSTRACT **We report the development of a fluorescence-based immunoassay technique relying on the physical phenomena of random number fluctuations and diffusion, which we review. By determining the autocorrelation of the fluctuations in the fluorescent intensity, this method is able to measure the amount of labeled antigen or antibody that is bound to micrometer-sized carrier particles in solution. The principal advantage of this technique is its insensitivity to small, fast-diffusing sources. It also discriminates against weakly fluorescent contaminants of size comparable to the carrier particles. We demonstrate these attributes by using two model systems: a human IgG assay and an idealized system consisting of polystyrene fluorescent spheres and rhodamine dye.**

Considerable effort has been devoted to the development of fluorescence-based immunoassay methods to replace the technique of radioimmunoassay for some routine clinical tests. The radioimmunoassay method is very powerful, owing to its high sensitivity and specificity. Its principal disadvantage is its reliance on expensive and potentially hazardous reagents that have a limited shelf life and whose use requires special handling and disposal procedures and expensive instrumentation.

Several fluorescence-based immunoassay techniques are currently in use or are undergoing clinical evaluation (1–4). This paper introduces an approach that relies on the existence of long-lived *correlations* of fluorescently labelled complexes in solution. Our preliminary results, as well as theoretical analysis, indicate that this correlation technique inherently possesses high sensitivity.

Our assay is an adaptation of a technique developed by Weissman *et al.* (5) to determine the molecular weight of DNA molecules (10^8 to 10^{11}) by using fluorescent dye binding. The ultimate goal of the technique is to measure the concentration of complexes Ag–Ab* or Ag*–Ab, which fluoresce due to labeled antigen (Ag*) or antibody (Ab*) while remaining insensitive to the presence of unbound fluorescing molecules in solution (in particular, free Ag* or Ab*). The key to the method is the requirement that the immunological reaction of interest occur on the surfaces of large "carrier" particles (e.g., micrometer-sized acrylamide gel, polystyrene latex, etc.).

The technique of Weissman *et al.* (5) relies on two physical phenomena: number *fluctuations* of particles within a prescribed volume in solution due to random Brownian motion, and *diffusion* of particles, in which the diffusion coefficient is inversely related to particle size. To distinguish between large, slowly diffusing sources of fluorescence (due to Ag*–Ab or Ab–Ab* attached to carrier particles) and small, rapidly diffusing ones, we simply keep track of the fluctuations in fluorescence intensity that occur for a given small volume element in the solution. Clearly, any fluctuation in intensity that occurs due to a fluctuation in the number of particles present in the volume will, on average, persist for a time which depends inversely on the rate of diffusion of the particles into or out of the sampling volume. For the large tagged carrier particles these fluctuations will be very long lived. For any small, freely diffusing fluorescing molecules there will effectively be no "memory" of a fluctuation having occurred at a finite time earlier, provided that the sampling volume is made appropriately small.

THEORY

Let us assume that the solution contains N identical fluorescing particles per sampled volume δV. At any instant the number of particles in δV will fluctuate according to Poisson statistics; the root mean square magnitude of the fluctuations is $N^{1/2}$. A convenient way to monitor these fluctuations is to evaluate the familiar intensity autocorrelation function,

$$C(t) = \langle I(t') \cdot I(t' - t) \rangle_{t'} \qquad [1]$$

in which $I(t')$ is the fluorescent intensity originating from δV at time t' and the symbol $\langle \cdots \rangle_{t'}$ indicates an average of the intensity product over a large number of sampling times t'.

We now periodically sample the fluorescent intensity at hundreds of locations within the solution, using in each case a volume of the same size ($\delta V \approx 10^{-6}$ cm^3). The large number of samples increases the signal/noise ratio of function $C(t)$. When time t equals an integral multiple of the repetition period T, the two intensities that form the product in Eq. 1 refer to the same volume element, for a given t'. The usefulness of the autocorrelation function in our application depends upon the fact that a number fluctuation in δV has a finite lifetime, τ. Fig. 1*a* is an idealized trace of the intensity $I(t')$ showing two fluctuations, each of which repeats after the period T ($\tau \gg T$). In reality, the intensity fluctuations do not resemble the regular, symmetric pattern of Fig. 1*a*; rather, they appear as "random" noise (as illustrated in Fig. 2). This idealization was chosen to permit a simple algebraic computation of $C(t)$ as discussed below. We assume a mean number of particles N per volume δV, each particle fluorescing with intensity I, giving a mean intensity $I \cdot N$. For simplicity we arbitrarily choose a positive and a negative fluctuation in intensity, with the size of each fluctuation given by the root mean square value, $I \cdot N^{1/2}$. Due to the deliberate physical overlapping of the sampling volumes in solution, there is a finite perisistence width $\Delta t'$ of the fluctuations in Fig. 1*a*.

We now evaluate $C(t)$ for the $I(t')$ shown in Fig. 1*a*, averaging the time t' over one period for convenience. Computing

The publication costs of this article were defrayed in part by page charge payment. This article must therefore by hereby marked "*advertisement*" in accordance with 18 U. S. C. §1734 solely to indicate this fact.

† On leave from Department of Physics, Colby College, Waterville, ME 04901.

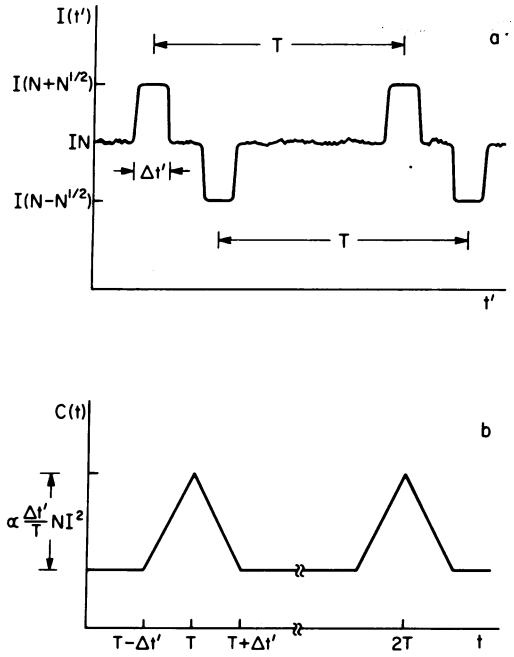

FIG. 1. Idealized trace of the intensity in time (*a*) and the resulting autocorrelation function versus the separation time (*b*).

$C(t)$ for the special case $t = T$, the scanning period, clearly maximizes $C(t)$, yielding

$$C(T) = \frac{\Delta t'}{T}[I^2(N + N^{1/2})^2 + I^2(N - N^{1/2})^2] + \frac{T - 2\Delta t'}{T} I^2N^2$$

$$= I^2N^2 + 2\frac{\Delta t'}{T} I^2N. \quad [2]$$

Calculating $C(t)$ for separation times t substantially different from T (i.e., $t < T - \Delta t'$ or $t > T + \Delta t'$ but t not near $2T$, $3T$, etc.) gives $C(t) = I^2N^2$. This is simply the square of the mean intensity and forms the uncorrelated part of Eq. 2 (i.e., the baseline). Fig. 1*b* shows the resulting $C(t)$ computed for all times t. Thus, when the fluctuation lifetime τ is much greater than T, the height P of the correlation peak above the uncorrelated baseline is given by

$$P \propto \frac{\Delta t'}{T} N \cdot I^2. \quad [3]$$

Next we explicitly consider a two-component system: N_b *b*-type particles, each of intensity I_b, plus N_f *f*-type particles of "unit" intensity, per volume δV. (I_b is the number of *f*-type intensity units on each bead.) Subscript *b* denotes fluorescence *bound* to large carrier particles, and subscript *f* denotes the fluorescence due to *free* molecules. Assuming statistical independence of the two species, we obtain from Eq. 3 the dependence of the correlation peak height on the above parameters,

$$P \propto (N_bI_b^2 + N_f) \quad [4]$$

in which it is assumed that fluctuation lifetimes τ_b and τ_f are both much greater than the period T. If $N_bI_b^2 \gg N_f$, the correlation peak height is almost entirely due to the fluctuations of *b*-type particles, in which case measurement of P then allows the relative determination of either N_b or I_b. Even when the average fluorescent intensity due to *b*-type particles is comparable to that of the *f*-type particles (i.e., $N_bI_b \approx N_f$), the *b*-type particles can dominate in the correlation result if they are bright enough (i.e., if I_b is large enough).

We can significantly enhance the detection of bright *b*-type particles relative to weak *f*-type sources if the fluctuation lifetime τ_b happens to be much longer than τ_f. This will be the case if the *b*-type particles are much *larger* than the *f*-type particles, provided that *diffusion* is the dominant effect governing the motion of these particles. Then the period T can be chosen such that $\tau_f \ll T \ll \tau_b$, resulting in no "memory" of *f*-type fluctuations occurring in a given volume δV at a time $t = T$ later, regardless of the relative magnitudes of the two types of fluctuations. Effectively this means that N_f can be set equal to zero in Eq. 4.

Diffusion causes a number fluctuation Δn in a cubic volume of dimension ℓ to relax exponentially with a diffusional lifetime given by

$$\tau_D \cong \ell^2/14 \cdot D \cong \frac{1.3\eta\ell^2}{kT} R_h. \quad [5]$$

We have used the Stokes–Einstein equation to relate the diffusion coefficient D to the particle hydrodynamic radius R_h; η is the solvent viscosity, k is Boltzmann's constant, and T is the absolute temperature. Eq. 5 is an estimate of the diffusional lifetime of a fluctuation that is centered in the (cubical) sampling volume. Clearly, in general there will be a distribution of decay lifetimes due to the spatial distribution of fluctuations within the volume. For geometries other than a cube, a similar result is obtained, with a different numerical factor. Taking ℓ to be approximately 100 μm, we find that, at room temperature in water, the diffusional lifetime of number fluctuations for particles of radius R_h (in μm) is

$$\tau_D \text{ (sec)} \approx 3000\, R_h. \quad [6]$$

Of course, the occurrence of velocity currents in solution may impose a significantly lower limit on the fluctuation lifetimes of all species. Nevertheless, a significant result is obtained if there are two radically different sizes of fluorescing particles in solution, with the fluctuation lifetime of the smaller species diffusion limited. In that case, one can design an immunoassay which is highly sensitive to fluorescence bound to large particles but quite insensitive to fluorescing molecules that are part of the fast-diffusing "background."

EXPERIMENTAL APPARATUS

A simplified diagram of the fluorescence-fluctuation spectrometer is shown in Fig. 2. Pinhole P (diameter, 100 μm) is used to define the beam of light incident on the sample cell S. It was convenient to use an argon-ion laser, $\lambda = 488$ nm (blue), to excite the fluoresein isothiocyanate-labeled molecules. Coherence of the light source is *not* required—any suitably filtered incandescent source would suffice.

Any labeled molecules that lie within the pencil beam volume defined by P will emit fluorescent light. Lens L projects this line image onto a photographic slit S at the face of the photomultiplier detector *PMT*. Filter F (Corning no. 3–69) blocks the 488-nm blue exciting light scattered from particles in solution, leaving the yellow-green fluorescein emission plus any long wavelengths emitted by fluorescing impurities. The width of slit S is also 100 μm. Thus, an effective illuminated/detected volume δV of the order of 10^{-6} cm^3 is defined by these optics.

As described thus far, the approach is identical to that used successfully by Weissman *et al.* (5) for DNA size determination. The significant change in design occurs in the choice of the means of periodically sampling the intensity as a function of

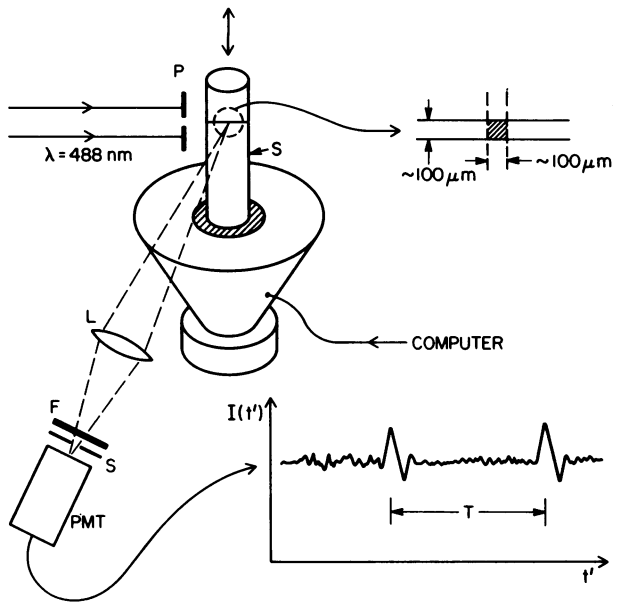

FIG. 2. Schematic of the experimental arrangement showing the sample cell S, vertically translated, in which the volume $\delta V \approx 10^{-6}$ cm^3 is defined by the associated optics.

position within the sample solution. In the original DNA study a cylindrical sample cell was uniformly rotated ($T \approx 5$ sec) by a slow-speed synchronous motor and drive belt. Instead, we used a *linear* translation scheme. The sample cell is a cylindrical tube that is uniformly translated in an up/down vertical motion by using a loudspeaker. Two sizes (outside diameter) of tubes were used in these experiments: 6-mm disposable culture tubes and 2-mm 100-μl micropipets. These tubes were centered within a standard 1-cm fluorimeter cuvette filled with water for the purpose of index-matching the incident light beam to minimize stray reflections. Sample solution volumes as small as 20 μl are easily achieved in the small tubes.

The sample tube is translated up to 0.8 cm according to a triangular waveform, with the period adjustable from 0.2 to 20 sec. The triangular driving waveform in reality consists of a rising and falling staircase of discrete steps, adjustable in number from 64 to 1024. Each step corresponds to a discrete time bin of width δt used to approximate the autocorrelation function $C(t)$ of Eq. 1. Typical values of δt range from 1 to 10 msec. An important innovation is the use of a microcomputer (Motorola 6800) to synchronize the sample position with the time base used to form $C(t)$. Hence, the sample cell is "locked" into the autocorrelation time base and performs perfectly periodic motion. The run time can be arbitrarily long, with no short-term "jitter" or long-term slippage of position with time, thereby enhancing the sensitivity of the instrument to very weak intensity fluctuations.

The *PMT* photocurrent is converted to a voltage, with adjustable gain, dc offset, and filter time constant. This allows the signal to be optimally matched to the input range of a 4-bit analog-to-digital converter. In the instrument, successive 4-bit × 4-bit multiples are used by the microcomputer to form the autocorrelation function.

In addition to displaying the contents of the correlation channels on an oscilloscope, the microcomputer determines the baseline and the correlation peak height. These values are normalized by the number of sample intervals in the elapsed run time. In practice one scans the solution until the normalized peak height settles to a constant value—i.e., when $C(t)$ is well determined.

RESULTS

Human IgG Model System. For this series of experiments we utilized the Immunofluor reagents supplied by Bio-Rad Laboratories. These consist of human IgG molecules, which we refer to as the antigen, Ag; rabbit antibody to human IgG (i.e., anti-immunoglobulin) which has been tagged with fluorescein isothiocyanate, Ab*; and 3- to 5-μm-diameter acrylamide gel beads to which antibody molecules, Ab, are covalently bound. We denote the latter by the symbol Ab_b, b denoting binding to the carrier particle.

To perform this particular assay, known amounts of the antigen, IgG, were added to solutions of carrier particles (10^7–10^8 beads per cm^3). During incubation the antigen binds to the acrylamide particles. Each solution was then flooded with an excess of tagged antibody, nAb*, resulting in the reaction

$$n\text{Ab}^* + \text{Ab}_b + \text{Ag–Ab}_b \rightleftharpoons (n-1)\text{Ab}^* + \text{Ab}_b + \text{Ab}^*\text{–Ag–Ab}_b. \quad [7]$$

At this point the standard fluorimetric intensity assay consists of spinning down the acrylamide particles (to which are bound the complexes Ab*–Ag–Ab_b), discarding the supernatant, and measuring the mean fluorescent intensity, which should be proportional to the initial IgG concentration.

Our first test was to compare the results based on the correlation measurement with those of fluorimetry. For both methods the fluorescent "signal" is plotted in arbitrary units versus IgG concentration (μg/ml) (from dilutions of an IgG standard, 3200 mg/dl) (Fig. 3). For the fluorimetric assay (curve B) that signal is simply the mean intensity. For the correlation assay (curve A) the signal is the square root of the peak height (Eq. 4); N_b is the mean number of carrier particles in δV and I_b equals the number of fluorescing complexes, Ab*–Ag–Ab_b, per particle. N_b should be fixed; I_b is the unknown to be measured. Because we discard the free Ab* in solution, N_f should be zero. The correlation result closely parallels the simple measurement of total intensity. Both methods saturate at moderately high IgG concentrations, where a substantial fraction of the active antibody sites Ab_b have become occupied by IgG. Furthermore, at very high IgG levels both methods display a curious reverse behavior, in which presumably the

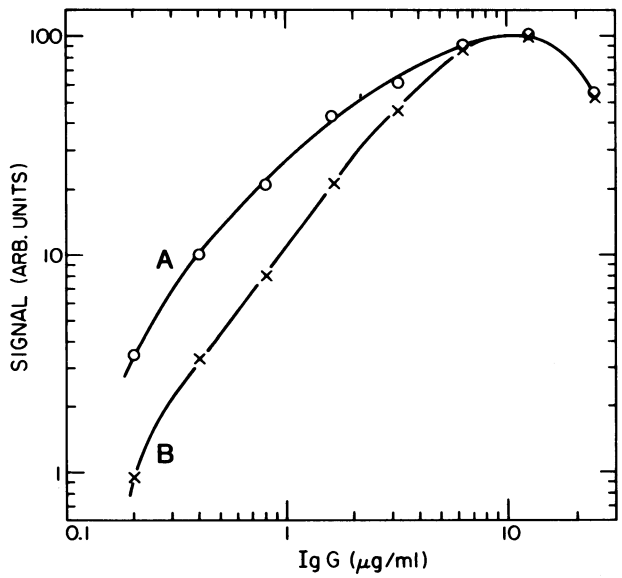

FIG. 3. Measured signal (in arbitrary units) versus the IgG concentration. Curve A gives the correlation result ($P^{1/2} \propto N_b^{1/2} I_b$); curve B gives the fluorimetry result (average intensity $\propto N_b I_b$).

number of available Ab_b sites on the carrier particles has been reduced due to substantial aggregation of the gel particles, promoted by the divalent IgG molecules.

Unlike fluorimetry, our assay is particularly sensitive to the formation of aggregates of the carrier particles. These aggregates occur because the divalent IgG crosslinks two Ab_b molecules belonging to two different carrier particles: Ab_b–Ag–Ab_b. The formation of aggregates increases the fluorescent intensity per carrier (I_b in Eq. 4) while proportionately decreasing the number of carriers per volume δV (N_b). Because the correlation peak height scales like $N_b I_b^2$, the formation of aggregates will enhance the signal. This is probably the cause of the "bowedness" of the correlation assay data shown in Fig. 3. (Computer simulations support this conclusion.)

The ability of the correlation assay to determine the amount of IgG bound to the carrier particles in the presence of varying amounts of free Ab* was also investigated. From Eq. 6 we estimate the diffusional lifetime of the 4-μm-diameter acrylamide beads to be roughly 6000 sec. The corresponding lifetime for the Ab* molecules was deduced from dynamic light scattering‡ to be approximately 25 sec.

In order to use diffusion to discriminate against the free Ab*, one should use a scanning period T of the order of 100 sec. However, we found that the fluctuation lifetimes of all species, large and small, were limited to about 10 sec, presumably due to velocity currents in the sample. These currents may be partially a consequence of the accelerations set up due to the up/down motion of the sample cell and partially due to thermal gradients. Hence, for the IgG experiments a short repetition period T was required (we used 1.2 sec); consequently, the contribution of the free Ab* to the correlated peak height could not be avoided.

Curve A in Fig. 4 is a plot of the correlation result (expressed in relative units) as a function of the amount of free tagged antibody Ab*, normalized to the bound intensity. The units of the x axis thus are $N_f/N_b I_b$ obtained by measuring mean fluorescent intensities (i.e., $N_f + N_b I_b$ and $N_b I_b$). In this test we kept the IgG concentration and the carrier particle density fixed. From curve A we see that, when the background free fluorescence is 10 times the carrier particle fluorescence, there is virtually no change in the correlation result for bound fluorescence. Thus, we have confirmed experimentally that the correlation assay does achieve a level of selectivity even when both fluorescing species are large and have long enough lifetimes to contribute to the correlation. The fact that the correlated signal increases at high Ab* concentrations demonstrates that the fluctuations of Ab* are indeed being correlated.

It is instructive to use the results of curve A to estimate the mean number of fluorescent complexes bound to a carrier particle. Eq. 4 shows that the correlation result, $P^{1/2}$, will increase by $2^{1/2}$ when $N_b I_b^2 = N_f$. Because the x axis is given by $N_f/N_b I_b$, the corresponding x axis value is I_b. From Fig. 4 we estimate that $I_b \approx 31$. The IgG concentration used in establishing curve A was 3.2 μg/ml. According to Fig. 3, this IgG level corresponds to approximately 33% saturation. Hence, we estimate a maximum of $\approx$100 fluorescent complexes per carrier particle (Bio-Rad Laboratories estimated 1000 antibodies per bead, of which 12–15% are active).

Finally, it should be mentioned that curve A does not strictly follow the response predicted by Eq. 4, if I_b is to remain constant at all Ab* concentrations. We believe that the discrepancy

‡ We filtered the scattered light (incident, λ = 488 nm) with a blue filter to remove the fluorescent light. A 4-bit autocorrelator was used to determine the mean diffusion coefficient (see ref. 6). Given an estimated molecular weight of 150,000 for Ab*, we conclude that Ab aggregates are common.

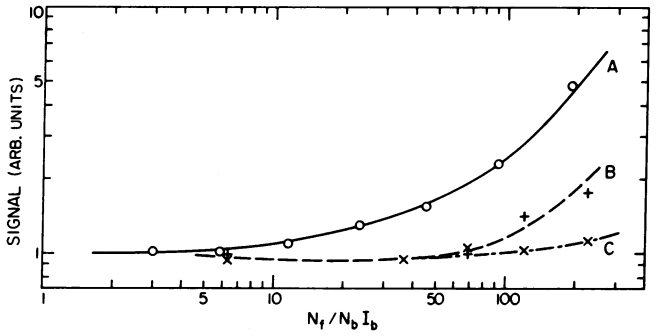

FIG. 4. Relative correlation signal, $P^{1/2} \propto (N_b I_b^2 + N_f)^{1/2}$, versus the ratio free fluorescence/bound fluorescence (equal to $N_f/N_b I_b$). Curve A, system acrylamide bead–Ab_b–Ag–Ab* + Ab*; curves B and C, polystyrene fluorescent spheres + rhodamine, at T = 1.2 sec and T = 10.2 sec, respectively.

is explained by a decreasing I_b, perhaps due to the increasing likelihood of the reaction

$$Ab_b\text{–Ag–Ab*} + Ab^* \rightleftharpoons Ab_b + Ab^*\text{–Ag–Ab*} \qquad [8]$$

as the concentration of Ab* increases.

Idealized Model System. We next devised an experiment in which the fluctuation lifetime of the smaller ("free") fluorescing species is diffusionally limited. To achieve this we used commercially available fluorescent spheres (Duke Scientific, no. 267 diameter, 4.3 μm) for the large species and the dye rhodamine 6G for the fast-diffusing species. The latter has a molecular weight of 530 with an estimated hydrodynamic radius of 6.7 Å (based on a globular molecule of protein-like density). For this series of experiments we attempted to reduce flow currents due to sample motion plus thermal gradients by drastically reducing the sample cell diameter. For the cell we used a portion of a standard 100-μl micropipet (1.3 mm inside diameter), resulting in an active solution volume of less than 20 μl. This was centered in a fluorimeter cuvette filled with water for index matching as well as thermal sinking. From an analysis of the resulting fluctuating signals, we concluded that use of the small-diameter tube coincidentally reduced the volume δV by a factor of 3, due to the focusing lens effect of the glass tube. The resulting diffusional relaxation times out of this reduced volume for the polystyrene spheres and the rhodamine 6G are estimated, from Eq. 5, to be about 3000 and 1.0 sec, respectively. Thus, we expect that scanning periods T on the order of 10 sec should allow us to discriminate effectively against the background fluctuations of the rhodamine 6G, whereas at T = 1 sec we expect only marginal discrimination.

Curves B and C in Fig. 4 are plots of the relative correlated signal as a function of the ratio of free to bound fluorescence for T = 1.2 and 10.2 sec, respectively. In both cases, the insensitivity to the "free" fluorescence is better than in curve A. This result could be explained by assuming that the fluorescent polystyrene spheres are more fluorescent relative to the free species (i.e., that I_b is a larger number) than are the Ab*–Ag–Ab_b complex-coated particles of curve A. However, rhodamine 6G molecules do correlate less efficiently at longer repetition periods than do the free Ab* molecules, owing to the fact that the former diffuse faster than the latter by 1 order of magnitude. The significance of this difference is seen by comparing curves B and C. The latter curve is essentially flat all the way out to a free fluorescence intensity 200 times larger than the bound value. This is our principal result. It clearly demonstrates the high level of insensitivity of this technique to fast-diffusing sources of fluorescence.

DISCUSSION

Detailed comparison of this fluorescence correlation assay with the radioimmunoassay (as well as other fluorescence techniques) requires further testing on systems of clinical significance. In order to evaluate the practical sensitivity of the proposed method it is necessary to consider the level of fluorescent contamination. For the case in which there is negligible background contamination, the correlation technique is no more sensitive than a simple measurement of total intensity. For example, in our IgG model assay we are able to detect approximately 1 fluorescent complex per carrier particle, which corresponds to a concentration of 10^7–10^8 labeled molecules per cm^3. However, the correlation method retains sensitivity in situations in which there is a background of fluorescent sources. We have demonstrated (curve C of Fig. 4) that this new method is highly insensitive to fast-diffusing background fluorescence. In straightforward intensity assays, unwanted small sources must be removed by a separation step (e.g., filtering, centrifugation, etc.). The correlation assay inherently provides a filter against small sources. We have also demonstrated a level of insensitivity to relatively large unwanted sources. In curve A of Fig. 4, both the labeled antibody molecules and the carrier beads contributed to the signal. The selectivity in favor of the carrier particles resulted from their relative brightness (i.e., their large I_b). Hence, in situations in which contaminants are individually much dimmer than, but of the same size as, the primary particles (i.e., size-based separation techniques would not work), this immunoassay technique would still be insensitive to the contaminants. From curve A and Fig. 4, we see that this insensitivity persists to somewhat beyond the point where the net fluorescent intensity of the contaminants is 10 times larger than that of the carrier particles (for $I_b - 30$).

A number of technological details influence the overall performance of this method. One of these is the bit resolution of the analog-to-digital converter; another is the scheme used for scanning the sample volume. We experimented with a scanning scheme in which the sample cell was kept stationary, but we encountered troublesome artifacts in the signal due to optical limitations. Although the overall performance of the assay method may be improved by further attention to these details, we believe that sample-related factors will provide the ultimate limitation. For example, in our IgG experiments we experienced difficulties associated with carrier particle aggregation. In other assay systems one may encounter large-particle fluorescent contamination. In summary, we have already demonstrated the potentially high sensitivity of this new technique. It remains to be determined whether this method offers a fundamental improvement for fluorescence-based immunoassays.

We thank G. Feher for useful suggestions regarding the experimental method and the manuscript, D. Sears for helpful conversations concerning immunology, and D. Pfost for help in constructing the microprocessor-based autocorrelator. This work was supported by a grant from the National Institutes of Health (5 R01 AI 15073-02) as well as funding from the campus research committee of the University of California, Santa Barbara.

1. Burgett, M. W., Fairfield, S. J. & Monthony, J. F. (1977) *J. Immunol. Methods* **16**, 211–219.
2. Kronick, M. N. & Little, W. A. (1975) *J. Immunol. Methods* **8**, 235–240.
3. Watson, R. A. A., Landon, J., Shaw, E. J. & Smith, D. S. (1976) *Clin. Chim. Acta* **73**, 51–55.
4. Dandliker, W. B., Kelly, R. J., Dandliker, J., Farquhar, J. & Levin, J. (1973) *Immunochemistry* **10**, 219–227.
5. Weissman, M., Schindler, H. & Feher, G. (1976) *Proc. Natl. Acad. Sci. USA* **73**, 2776–2780.
6. Chu, B. (1974) *Laser Light Scattering* (Academic, New York).